Magnetic phase transitions in a random mixture with competing Ising and XY spin anisotropies

K. Katsumata
Research Institute of Applied Electricity, Hokkaido University, Sapporo 060, Japan

J. Tuchendler*
Laboratoire des Propriétés Mécaniques et Thermodynamiques des Matériaux, Université Paris Nord, Avenue J. B. Clément, 93430 Villetaneuse, France

S. Legrand
Direction de la Physique Générale, Service de Résonance Magnétique, Centre d'Etudes Nucléaires de Saclay, B.P.2, 91190 Gif-sur-Yvette, France
(Received 17 January 1984)

Magnetic phase transitions in the randomly mixed antiferromagnet $Fe_{1-x}Co_xBr_2$ with competing Ising and XY anisotropies have been studied experimentally by ac-susceptibility and magnetization measurements. The concentration—versus—transition-temperature phase diagram of this alloy under zero external magnetic field is constructed. The transition from the paramagnetic to antiferromagnetic phase was clearly observed in both the Fe- and Co-rich regions. One of the two low-temperature phase boundaries which corresponds to the ordering of the Ising component becomes less sharp. The other one, which represents the ordering of the XY component, is missing. The absence and the smearing of the transitions are discussed in the random field model. The effect of external magnetic field on the phase transition between the paramagnetic and antiferromagnetic phase has been studied in the Fe-rich region. The external field applied along the c axis of the crystal (the Ising axis) caused the transition to be smeared, and thus the external field produced a random field in this alloy as in the case of diluted antiferromagnets. From these experimental observations, the lower critical dimension of the Ising model is shown to be three.

I. INTRODUCTION

Magnetic phase transitions in randomly mixed crystals with competing spin anisotropies have been a subject of recent theoretical[1] and experimental[2] studies. Mean-field theories[3–6] have predicted the presence of three ordered phases, bounded by four critical lines, in the concentration—versus—transition-temperature phase diagram. The three phases are two antiferromagnetic phases, the properties of which are, as a whole, the same as those in respective pure materials, and a new phase called an "oblique antiferromagnetic" (OAF) phase,[4–6] or a "mixed ordering" (MO) phase.[7,8] Early renormalization-group calculations[7,8] by Aharony and Fishman have shown that these four critical lines meet at a "decoupled" tetracritical point. Katsumata *et al.*[9–11] have reported that the random mixture $Fe_{1-x}Co_xCl_2\cdot 2H_2O$ of two antiferromagnets, $FeCl_2\cdot 2H_2O$ and $CoCl_2\cdot 2H_2O$, with competing uniaxial spin anisotropies exhibits the tetracritical phase diagram. They have observed sharp anomalies at the four phase boundaries in both the susceptibility and specific-heat measurements. A recent neutron-scattering experiment[12] on the same system has demonstrated that the transition at the low-temperature phase boundary is as sharp as that at the high-temperature one.

A new effect is observed when a mixed system in which a uniaxial (Ising) and planar (XY) anisotropies are competing is studied.[13–18] A typical example of such system is the anhydrous mixture $Fe_{1-x}Co_xCl_2$ (Refs. 13–15 and 18). The easy axis of $FeCl_2$ points along the c axis of the crystal, while the Co spins in $CoCl_2$ are confined in the c plane and the anisotropy within the plane is very small. The concentration—versus—transition-temperature phase diagram of $Fe_{1-x}Co_xCl_2$ has been determined from susceptibility and neutron-scattering experiments.[13–15,18] The transitions at the two low-temperature phase boundaries in $Fe_{1-x}Co_xCl_2$ become less sharp compared with those at the high-temperature phase boundaries. Wong *et al.*[15,18] have argued that the random field coming from the nondiagonal exchange interactions in this mixed crystal causes the two low-temperature phase boundaries to become less sharp. Suppose we have a nondiagonal exchange interaction of the form $-2\tilde{J}_{ij}S_i^{\parallel}S_j^{\perp}$, where $S_i^{\parallel}$ is the spin component along the c axis at site i, $S_j^{\perp}$ is that in the c plane at site j, and $\tilde{J}_{ij}$ is site random. Here, we are discussing the case where the diagonal exchange interaction between Fe^{2+} and Fe^{2+} spins, that between Co^{2+} and Co^{2+} spins, and that between Fe^{2+} and Co^{2+} spins are larger than the nondiagonal exchange interactions. When, for example the $S^{\parallel}$ ordering is established at the transition from the paramagnetic to antiferromagnetic phase in the Fe-rich concentration region, a random field $\tilde{J}\langle S^{\parallel}\rangle/\mu_B$ acts on $S^{\perp}$, where $\langle\ \rangle$ denotes the thermal average. In the Co-rich region, the roles of the $S^{\parallel}$ and $S^{\perp}$ are reversed. It is widely accepted that in Heisenberg and XY systems a random field destroys the long-range order

below four dimensions.[19] In the case of Ising systems the situation is less clear. Whether the lower critical dimension (d_c) below which no long-range order exists is two or three is still controversial. Although both of the two low-temperature phase boundaries are less sharp in $Fe_{1-x}Co_xCl_2$, they are experimentally detectable. It seems difficult to explain this observation by the random-field model, since the effect of the random field on destroying the long-range order is stronger for XY systems than Ising ones for a given space dimensionality.

The purpose of this paper then, is, to clarify the nature of the phase transition in a randomly mixed system with competing Ising and XY anisotropies. The system chosen for this study is the mixture $Fe_{1-x}Co_xBr_2$. The main difference between $Fe_{1-x}Co_xBr_2$ and $Fe_{1-x}Co_xCl_2$ lies in that the former is less two dimensional than the latter. Preliminary results have been reported earlier.[20]

The format of this paper is as follows. In Sec. II we describe the crystal and magnetic properties of $FeBr_2$ and $CoBr_2$. The experimental details are given in Sec. III. In Sec. IV we present the concentration—versus—transition-temperature phase diagram of $Fe_{1-x}Co_xBr_2$ in zero external magnetic field obtained from the present experiment. In Sec. V the magnetization—versus—external-magnetic-field curves of this mixed system are given. We have studied the effect of an external magnetic field on the transition from the paramagnetic to antiferromagnetic phase in the Fe-rich concentration and on the transition at the low-temperature phase boundary. The results are given in Sec. VI. The last section is devoted to discussion.

II. CRYSTAL AND MAGNETIC PROPERTIES OF $FeBr_2$ AND $CoBr_2$

The compounds $FeBr_2$ and $CoBr_2$ have the crystal structure of CdI_2 ($P\bar{3}m$) shown in Fig. 1. The crystal has a layer structure. A sheet composed of the metallic ions is sandwiched by two Br^- sheets. The lattice parameters of $FeBr_2$ and $CoBr_2$ are shown in Table I. They differ from each other only slightly. Moreover, the ionic radii of Fe^{2+} and Co^{2+} are nearly the same. Thus, we expect that $FeBr_2$ and $CoBr_2$ make a good solid solution over the entire range of concentrations.

From the neutron-diffraction experiment,[21] both $FeBr_2$ and $CoBr_2$ are antiferromagnetic at low temperatures. The spin structures of $FeBr_2$ and $CoBr_2$ are such that spins in a c plane are coupled ferromagnetically, while they are coupled antiferromagnetically with the spins in the adjacent c planes. Spins in $FeBr_2$ point along the c axis, while they are confined in the c plane in $CoBr_2$. The Néel temperature of $FeBr_2$ has been determined from specific-heat measurements[22] to be 14.2 K, while that of $CoBr_2$ has been determined to be 19 K from neutron-scattering experiments.[21] Yelon and Vettier have determined the exchange and anisotropy parameters in $FeBr_2$ from the inelastic-neutron-scattering experiment.[23] The spin Hamiltonian they used is

$$\mathcal{H}=\sum_i D[(S_i^z)^2-\tfrac{2}{3}] + \sum_{i>j}[(-2/\eta)J_{ij}S_i^zS_j^z-2J_{ij}(S_i^xS_j^x+S_i^yS_j^y)], \quad (1)$$

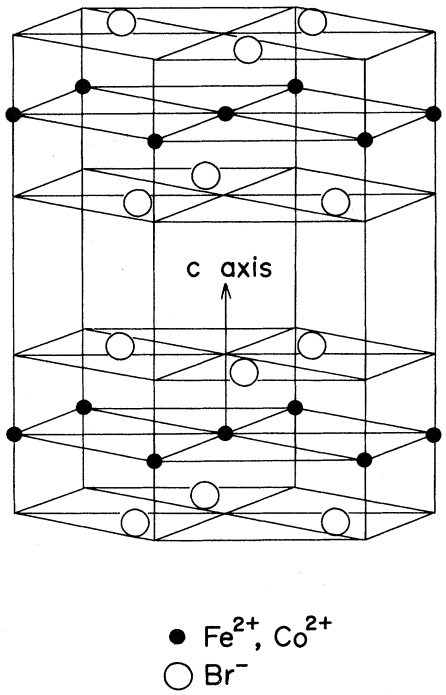

FIG. 1. Crystal structure of MBr_2 ($M=Fe^{2+}$ or Co^{2+}).

where $S=1$, D is a single-ion anisotropy parameter, J_{ij} is an isotropic exchange constant between spins, and the z axis is taken to be parallel to the c axis of the crystal. The parameter η represents the anisotropy in the exchange and is given by $\eta=g_x^2/g_z^2$, where g_z and g_x are, the g values along the c axis and c plane, respectively. The exchange constants they considered are J_1 (the nearest-neighbor exchange constant in the c plane), J_2 (the next-nearest-neighbor exchange constant in the c plane), and J_1' (the exchange constant between planes). The values of these constants are given in Table I. The anisotropy energy given by

TABLE I. The lattice parameters, Néel temperatures, parameters of the spin Hamiltonians, and transition fields of $FeBr_2$ and $CoBr_2$.

	$FeBr_2$	$CoBr_2$
Lattice parameters (Å)	$a=3.772$ $c=6.223$	$a=3.728$ $c=6.169$
T_N (K)	14.2	19
Parameters of the spin Hamiltonian (cm^{-1})	$2J_1=5.07$ $2J_2=-1.70$ $2J_1'=-2.00$ $g\mu_BH_A=14.28$	$J_1=16.2$ $J_2=0.15$ $D_1=9.20$ $J_3=-2.73$ $J'=-7.82$ $D_2=D_3=0$ $D'=-0.48$
Transition field at 4.2 K (kOe)	$H_c=31.5$	$H_s=74.2$

$$g\mu_B H_A = -D + [(1-\eta)/\eta][2J(0) - 2J'(0)] \quad (2)$$

has also been determined from experiment[23] and is shown in Table I. We see from Table I that $FeBr_2$ is not a good two-dimensional magnet and that the anisotropy energy is so large that $FeBr_2$ is well approximated by an $S=1$ Ising antiferromagnet. Yoshizawa *et al.* have determined the exchange parameters in $CoBr_2$ from the inelastic-neutron-scattering study.[24] They have used the following spin Hamiltonian with $S=\frac{1}{2}$:

$$\mathcal{H} = -\sum_{\text{NN}} (J_1 \vec{S}_i \cdot \vec{S}_j - D_1 S_{ix} S_{jx}) - \sum_{\text{NNN}} (J_2 \vec{S}_i \cdot \vec{S}_j - D_2 S_{ix} S_{jx}) - \sum_{\text{TNN}} (J_3 \vec{S}_i \cdot \vec{S}_j - D_3 S_{ix} S_{jx}) - \sum_{\text{NN}}{}' (J' \vec{S}_i \cdot \vec{S}_m - D' S_{ix} S_{mx}) . \quad (3)$$

The c axis of the crystal is taken as the x axis. The constants J_1, J_2, and J_3 in Eq. (3) are the nearest-neighbor (NN), next-nearest-neighbor (NNN), and third-nearest-neighbor (TNN) exchange constants in the c plane, respectively; D_i are the anisotropies in the exchange parameters, J' is the exchange constant between planes, and D' is the anisotropy in the exchange. Determined values are listed in Table I. We see that the compound $CoBr_2$ is a fairly good XY magnet. The space dimensionality of $CoBr_2$ is three rather than two. Thus, the mixed crystal $Fe_{1-x}Co_xBr_2$ serves as a prototype of a three-dimensional random alloy with competing Ising and XY anisotropies.

When an external magnetic field is applied along the c axis of $FeBr_2$ at low temperatures, a transition from the antiferromagnetic to ferromagnetic phase takes place[25–27] (metamagnetism). The value of the transition field is given in Table I. In $CoBr_2$, because the anisotropy in the c plane is very small, in the antiferromagnetic phase the spins point perpendicularly to the external magnetic field applied in the c plane. At high fields the spins point parallel to the magnetic field.[28] The value of the saturation field is given in Table I.

III. EXPERIMENTAL DETAILS

The single crystals of $Fe_{1-x}Co_xBr_2$ used in the present study were grown by a Bridgman method in Saclay. In most cases the boule contained a single crystal, and exhibited a perfect cleavage along the c plane. However, in a few cases the boule consisted of two or more single crystals. The concentrations of the mixture reported here are nominal ones. We have analyzed the concentrations of the $x=0.25$ and 0.40 crystals used in the present experiment by means of rf inductively coupled plasma atomic emission spectroscopy, and found that the concentrations coincide with the nominal ones within a few atomic percent.

The susceptibility measurements under zero external magnetic field were performed in Sapporo using an ac method. The apparatus is fully computerized using a Hewlett-Packard 9835A desktop computer. A Hewlett-Packard System 200-36A desktop computer was newly introduced either to serve as a back-up for the system or to analyze the data. The operating frequency of the ac field was 200 Hz. The samples used in the susceptibility measurement were disk-shaped platelets typically 5 mm in diameter and 1 mm thick. No attempt was made to correct the susceptibility values by taking into account the demagnetizing factor of the sample. This is not a serious problem in the present study since we are mainly concerned with the transition temperature. The temperature of the sample was measured by a Au(Fe)-Ag thermocouple, which was attached directly to the sample with Apiezon N grease. Another end of the thermocouple was immersed in a liquid-helium bath and the voltage across the thermocouple was measured by a digital nanovoltmeter (Takeda Riken TR-6515D/6018D or Keithley 181). The accuracy of the temperature at the sample position is estimated to be better than ± 0.05 K.

The magnetization measurements were performed in Sapporo using the magnetometer described earlier.[29] The sample was driven mechanically between two series-opposing pick-up coils with a frequency of 10 Hz. The ac signal from the pick-up coils was fed to a Princeton Applied Research 124A lock-in amplifier. The apparatus is fully automated by the use of the Hewlett-Packard computers. Magnetic fields were produced via a 60-kOe superconducting solenoid wound with Nb-Ti multifilamentary wire. When a weak magnetic field was needed, a solenoid coil wound with Cu wire cooled with liquid nitrogen was used. The temperature of the sample in this magnetometer was measured by a calibrated carbon-glass thermometer (Lake Shore Cryotronics, Inc.) which was placed close to the sample. The accuracy of the temperature at the sample position is estimated to be better than ± 0.001 K between 4.2 and 1.5 K and to be better than ± 0.5 K above 4.2 K.

IV. PHASE DIAGRAM

Figures 2(a)–2(f) show temperature dependences of the ac susceptibilities along the c axis ($\chi_{c\ \text{axis}}$) and c plane ($\chi_{c\ \text{plane}}$) of $Fe_{1-x}Co_xBr_2$ obtained in the Fe-rich concentration region. We see that for all of these concentrations the temperature dependence of the susceptibility is typical of a uniaxial antiferromagnet: The parallel susceptibility ($\chi_{c\ \text{axis}}$) shows a cusp and the perpendicular one ($\chi_{c\ \text{plane}}$) is almost temperature independent below the Néel point. Thus, the mixed crystal $Fe_{1-x}Co_xBr_2$ is in the antiferromagnetic phase at low temperatures for $x \leq 0.25$. The properties of this phase are the same as those of pure $FeBr_2$. The transition from the paramagnetic to antiferromagnetic phase is sharp in all of the concentrations, particularly in the $x=0.15$ and 0.25 samples. No indication of another phase transition is seen down to 4.2 K.

Figures 3(a)–3(f) show temperature dependences of the ac susceptibilities along the c axis and c plane of the mixed crystals with $x \geq 0.29$. In the concentrations 0.29, 0.325, and 0.40, an ordering of the spin component in the c plane takes place upon decreasing the temperature, followed by an ordering of the spin component along the c axis at lower temperatures. The phase transition at the

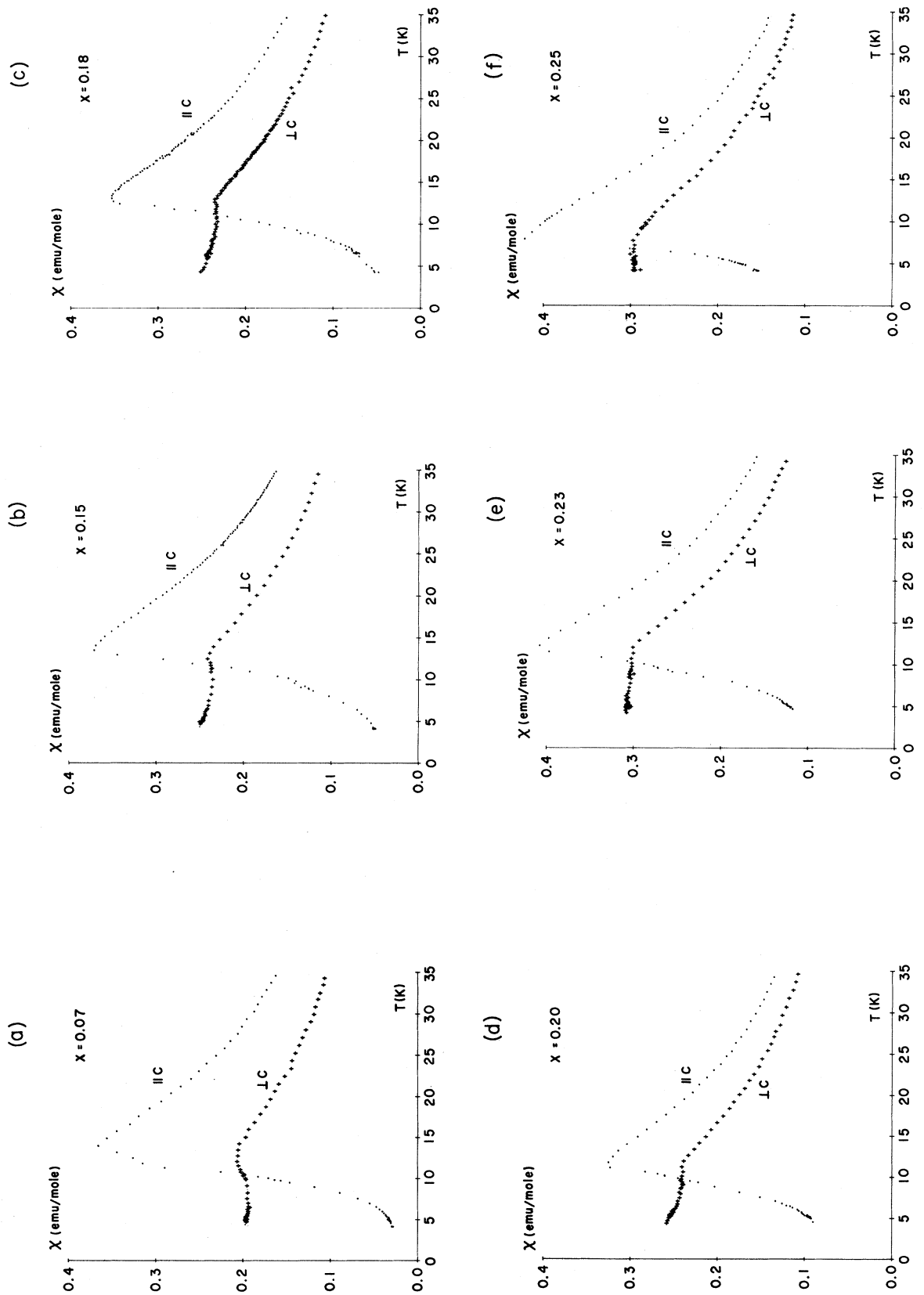

FIG. 2. Temperature dependences of the ac susceptibilities along the c axis (parallel to c) and in the c plane (perpendicular to c) of $Fe_{1-x}Co_xBr_2$ in the Fe-rich concentrations.

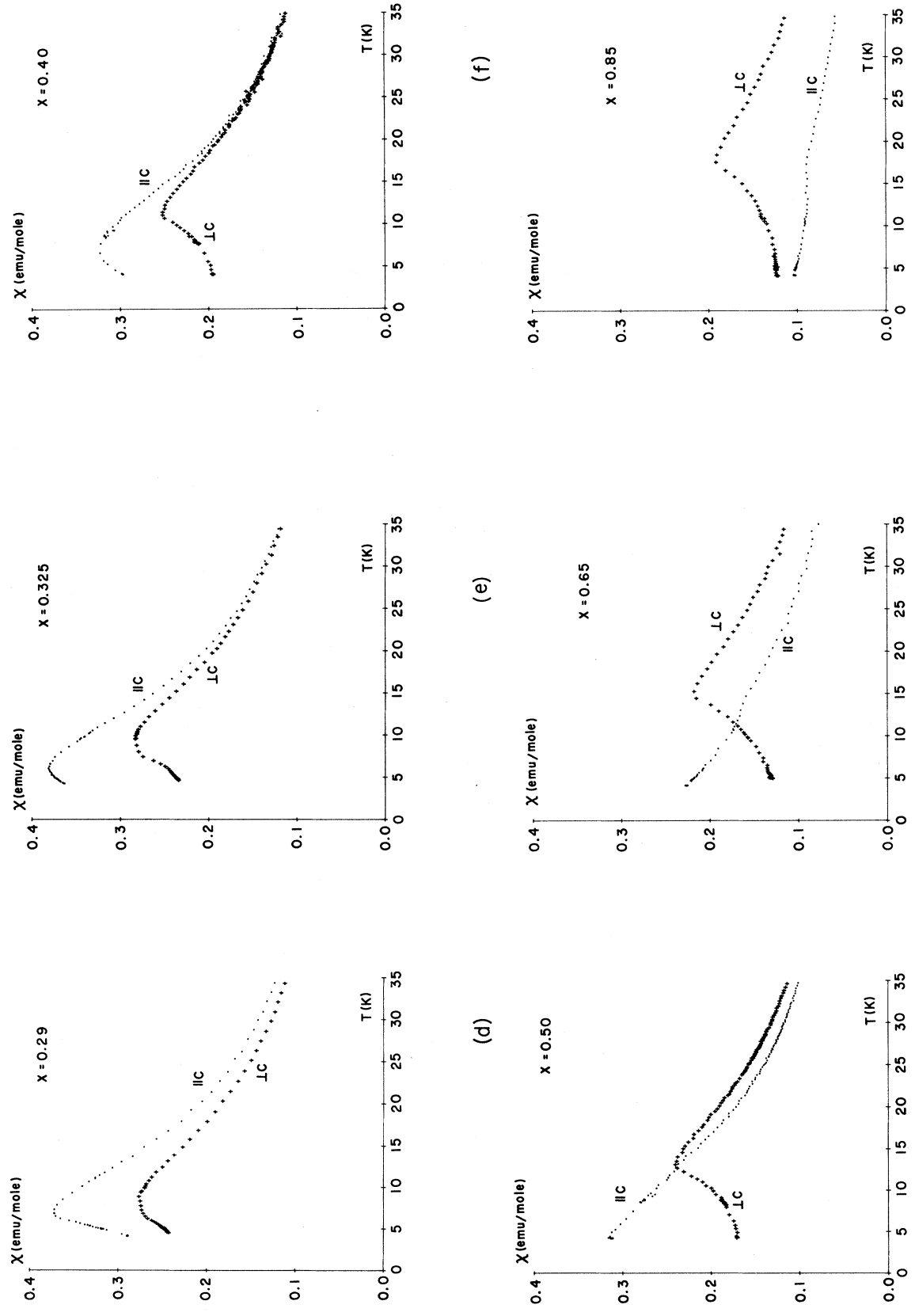

FIG. 3. Temperature dependences of the ac susceptibilities along the c axis (parallel to c) and in the c plane (perpendicular to c) of $Fe_{1-x}Co_xBr_2$ with $x \geq 0.29$.

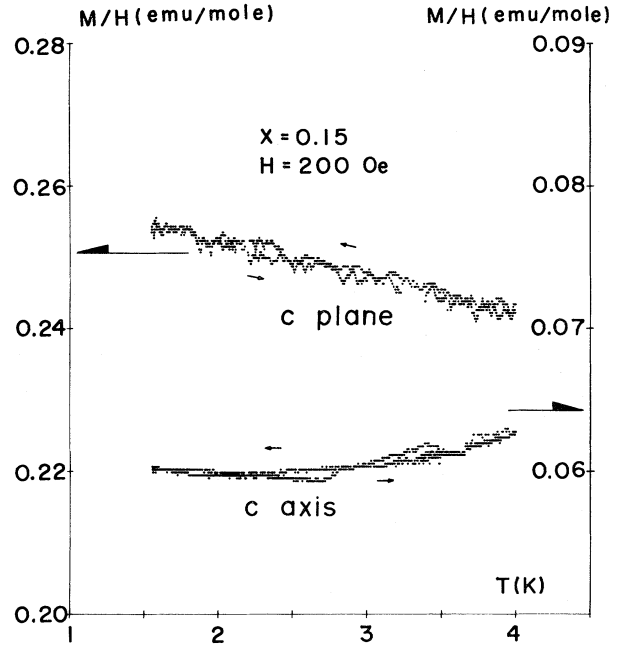

FIG. 4. Susceptibilities along the c axis and in the c plane of the $x=0.15$ sample plotted as functions of temperature below 4.2 K.

lower temperature is less sharp, as in $Fe_{1-x}Co_xCl_2$ (Refs. 13 , 15, and 18). For the concentrations 0.50 and 0.65, $\chi_{c\ \text{axis}}$ increases monotonically with decreasing temperature down to 4.2 K. In the $x=0.85$ sample, $\chi_{c\ \text{axis}}$ is almost temperature independent below T_N, indicating that the spins are confined in the c plane as in pure $CoBr_2$.

In order to obtain information about the low-temperature phase transition in the Fe-rich concentration region, we have measured temperature dependences of $\chi_{c\ \text{axis}}$ and $\chi_{c\ \text{plane}}$ below 4.2 K in the $x=0.15$ and 0.25 samples. In this experiment we have measured temperature dependences of the magnetization under a fixed external magnetic field by using the magnetometer described in Sec. III. The results are shown in Figs. 4 and 5. In the $x=0.15$ sample, $\chi_{c\ \text{plane}}$ increases slightly with decreasing temperature, and $\chi_{c\ \text{axis}}$ is almost temperature independent (note the difference in scale of the ordinate). The result shows that there is no indication of a low-temperature phase transition in the $x=0.15$ sample down to 1.5 K. In the $x=0.25$ sample, $\chi_{c\ \text{axis}}$ decreases monotonically with decreasing temperature, while $\chi_{c\ \text{plane}}$ is independent of temperature. Again, we have no indication of a low-temperature transition in this concentration down to 1.5 K.

The concentration—versus—transition-temperature phase diagram of $Fe_{1-x}Co_xBr_2$ obtained from the susceptibility measurements is shown in Fig. 6. The Néel temperature at respective concentrations was determined from the temperature at which the susceptibility is maximum. Precisely speaking, the Néel temperature determined in this way is slightly higher than the true one. The temperature at which the derivative of the susceptibility with respect to temperature, $d\chi/dT$, is maximum corresponds to a true T_N value.[30] However, in the Fe-rich concentration region, as $\chi_{c\ \text{axis}}$ is sharply peaked, the two ways of determining the Néel temperature give no significant difference. Also shown in Fig. 6 are the Néel temperature of $FeBr_2$ determined from the specific-heat measurement[22] and that of $CoBr_2$ obtained in the neutron-scattering experiment.[21] The phase diagram of this mixed system is, as a whole, similar to that of $Fe_{1-x}Co_xCl_2$ (Refs. 13—15 and 18): The Néel temperature in the Fe-(Co-) rich region decreases with increasing the number of Co (Fe) atoms. One of the two low-temperature phase boundaries which corresponds to the ordering of the Ising

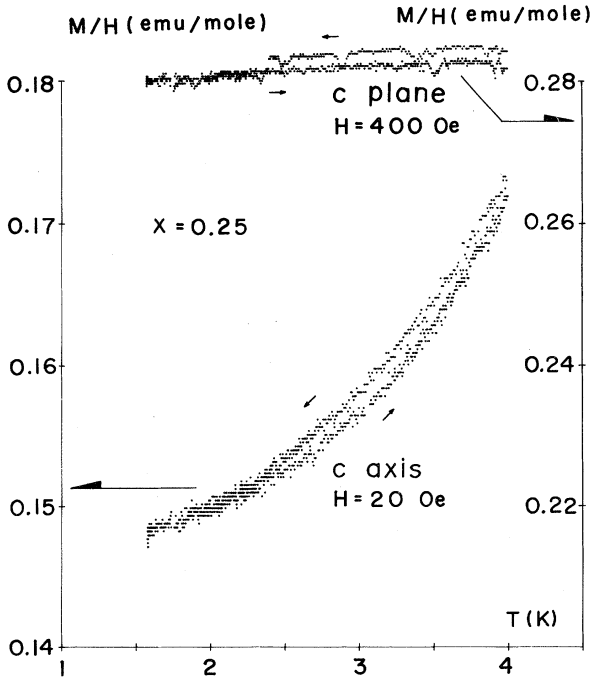

FIG. 5. Temperature versus susceptibilities along the c axis and in the c plane of the $x=0.25$ sample below 4.2 K.

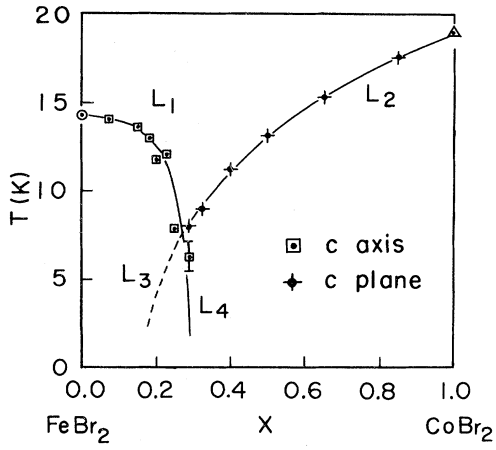

FIG. 6. Concentration—versus—transition-temperature phase diagram of $Fe_{1-x}Co_xBr_2$ obtained from the susceptibility measurements. Also shown in this figure are the Néel temperature of $FeBr_2$ determined from the specific-heat measurement (Ref. 22) and that of $CoBr_2$ obtained in the neutron-scattering experiment (Ref. 21).

component (L_4) is less sharp [Figs. 3(a)—3(c)], and the other one, which represents the ordering of the XY component (L_3), is missing. This last point is in contrast with the case of $Fe_{1-x}Co_xCl_2$, in which both of the low-temperature phase boundaries are experimentally observable, although they are broad. One might say that the line L_3 in Fig. 6 might not be a smooth extension of L_2, but might be located in the narrow region between $x=0.25$ and x_M (~ 0.28), where x_M is the multicritical concentration at which the critical lines L_1, L_2, and L_4 meet. However, in the case of $Fe_{1-x}Co_xCl_2$, $\chi_{c\ \text{plane}}$ begins to exhibit a broad peak below T_N when x_M is approached from zero, indicating the existence of the line L_3 (Refs. 13, 15, and 18), whereas $\chi_{c\ \text{plane}}$ of the $x=0.23$ and 0.25 samples show no such broad peak; rather they are almost temperature independent [Figs. 2(e), 2(f), and 5]. There are, in fact, a few examples of concentration—versus—transition-temperature phase diagrams in which the OAF, or MO, phase appears only in a very narrow concentration region. In the mixed system $K_2Mn_{1-x}Fe_xF_4$, the OAF phase is restricted to $0.02 \lesssim x \lesssim 0.03$ (Refs. 31 and 32), and in $CsMn_{1-x}Co_xCl_3 \cdot 2H_2O$ the OAF phase appears for $0.04 \lesssim x \lesssim 0.07$ (Ref. 33). In these systems, since the anisotropy energy of the Mn^{2+} spin is much weaker than that of the Fe^{2+} or Co^{2+} spin, only a small amount of Fe or Co atoms is sufficient to induce the Mn^{2+} spins to point parallel to the Fe^{2+} or Co^{2+} spins. Thus, not only is the concentration region at which the OAF phase exists very narrow, but the concentration region itself is located very close to $x=0$. This is not the case in the system studied here, as seen from Fig. 6. For these reasons we conclude that the line L_3 is missing in $Fe_{1-x}Co_xBr_2$.

V. MAGNETIZATION CURVE

We have measured isothermal magnetization curves in these mixed crystals at several selected concentrations. The results are presented in this section. These will be helpful to understand the effect of an external magnetic field on the phase transitions as reported in Sec. VI. The samples used in the magnetization measurements are the same as those used in the susceptibility measurements.

In Fig. 7 we show magnetic field dependences of the magnetization in the $x=0.15$ and 0.25 crystals. The magnetization curve in the $x=0.15$ sample is reminiscent of the metamagnetic transition observed in pure $FeBr_2$ (Refs. 25—27). The magnetization curve shows a hysteresis and thus the transition is still of first order as in pure $FeBr_2$. The transition region, at which the magnetization increases sharply with increasing magnetic field, is too wide to be explained by the demagnetizing field of the sample. The magnetization seems to almost saturate above 50 kOe. The value of the magnetization at 50 kOe is $3.38\mu_B$ per atom.

When we consider samples with a much larger concentration with Co^{2+}, the magnetization curve becomes gradual. From a careful inspection of the magnetization curve in Fig. 7, we see that the magnetization process in the $x=0.25$ sample takes place in three steps. At low fields, the magnetization increases slowly with field. In the region between about 10 and 30 kOe the magnetization grows considerably. Then, above about 30 kOe the change in the magnetization is again small. The transition region in the $x=0.25$ sample is wider than that in the $x=0.15$ crystal.

Figure 8 shows the magnetization curves in the $x=0.29$ sample. The magnetization changes slowly with magnetic field. There is little anisotropy in the magnetization curves.

Figure 9 shows an example of magnetization curve obtained in the Co-rich concentration. In the $x=0.50$ sample, the magnetization also increases slowly with magnetic field as in the $x=0.29$ crystal. We see an anisotropy in the magnetization curve at this concentration. It is easier to magnetize this sample along the c plane than to do it along the c axis. This means that the mixed crystal with this concentration has magnetic properties similar to those of pure $CoBr_2$. This observation is consistent with the phase diagram (Fig. 6) obtained in zero field.

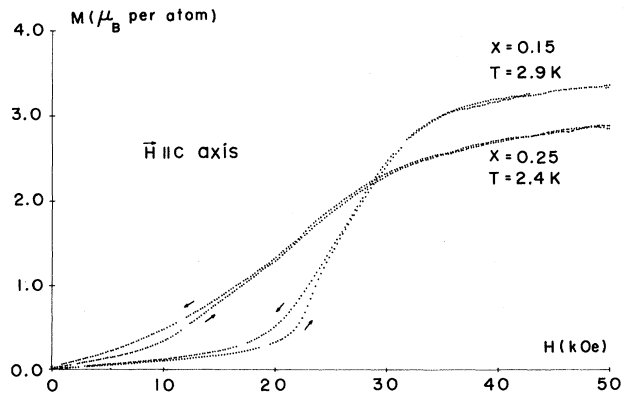

FIG. 7. Magnetization curves of the $x=0.15$ sample obtained at $T=2.9$ K and of the $x=0.25$ crystal observed at $T=2.4$ K. The external field was applied along the c axis. The magnetic field was varied with a speed of 120 Oe/sec.

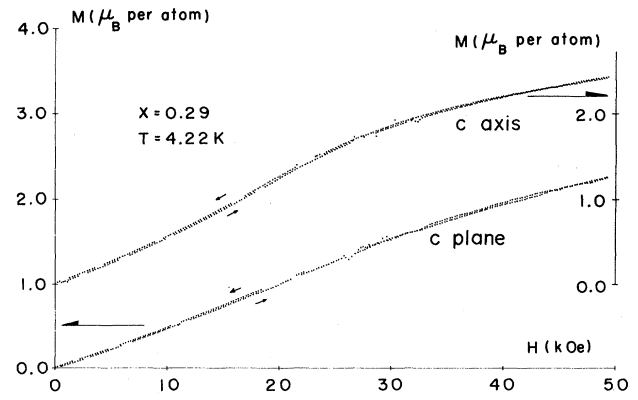

FIG. 8. Magnetization—versus—magnetic-field curves along the c axis and c plane of the $x=0.29$ sample obtained at $T=4.22$ K.

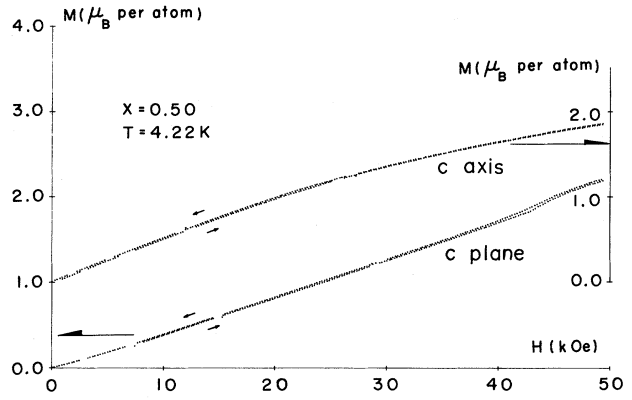

FIG. 9. Magnetic field dependences of the magnetizations along the c axis and in the c plane of the $x=0.50$ crystal obtained at $T=4.22$ K.

VI. EFFECT OF EXTERNAL MAGNETIC FIELD ON THE PHASE TRANSITIONS

In 1979, Fishman and Aharony[34] showed that a uniaxial antiferromagnet randomly diluted with nonmagnetic ions placed in a uniform external magnetic field behaves like a ferromagnet in a random uniaxial magnetic field. Since then, a number of experiments have been performed on the site-diluted antiferromagnets to test the theoretical predictions about the random-field effect.[19] According to Fishman and Aharony,[34] the random field comes from the randomness in the exchange interactions between spins. We therefore expect that a random field is present in our alloy in the Fe-rich concentration region when the external field is applied along the c axis. The strength of the random field in this antiferromagnetic mixture may be smaller than that in a site-diluted antiferromagnet, because the randomness in the exchange is smaller in the former than in the latter.

We have studied the effect of external magnetic field on the phase transition from the paramagnetic to the antiferromagnetic phase in the $x=0.25$ sample and on the low-temperature transition in the $x=0.29$ sample. In this experiment we have measured temperature dependences of the magnetization under fixed external fields. The result for the $x=0.25$ crystal is shown in Figs. 10(a) and 10(b). When the external magnetic field is very small, the susceptibility is sharply peaked. Upon increasing the magnetic field, the susceptibility-versus-temperature curve becomes rounded. Therefore, the external magnetic field indeed makes the phase transition in this mixed system less sharp, as expected. The Néel temperature, determined from the temperature at which the susceptibility is maximum, increases with increasing magnetic field up to about 5 kOe. Then T_N begins to decrease with the increase of the external field up to about 20 kOe. Above about 25 kOe, the susceptibility decreases monotonically with increasing temperature. The initial increase of T_N with magnetic field seems to be incompatible with the idea of the random-field effect, since the external field will destroy the long-range order and hence T_N should decrease with magnetic field. We explain this as follows: In our mixed crystal the uniaxial anisotropy of $FeBr_2$ and the planar anisotropy of $CoBr_2$ are competing. The decrease of T_N with Co concentration in the Fe-rich region of the phase diagram (Fig. 6) results from this competition. The external magnetic field applied along the easy-magnetization axis of $FeBr_2$ will help the ordering. Thus, T_N increases with external magnetic field. Although the

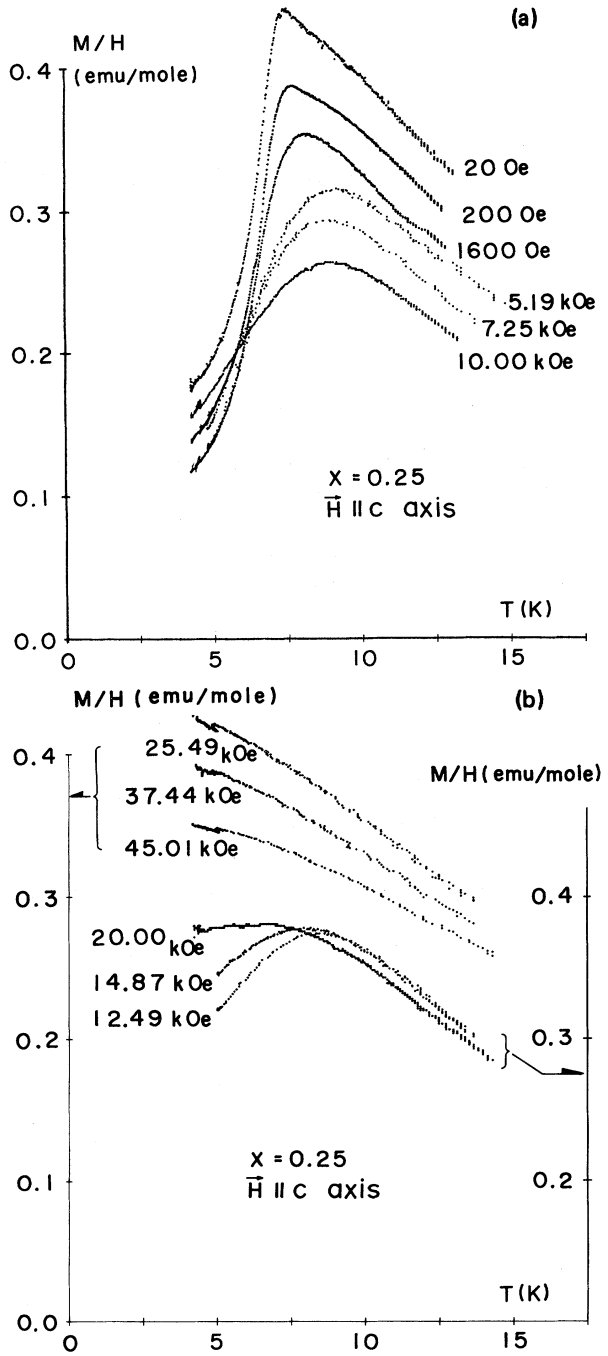

FIG. 10. Temperature dependence of the susceptibility along the c axis of the $x=0.25$ sample obtained under fixed external magnetic fields. In (a) the baseline of the susceptibility is down-shifted by 0.02 emu/mol for each field, for clarity. The baseline for the $H=20$ Oe curve is shown in the figure.

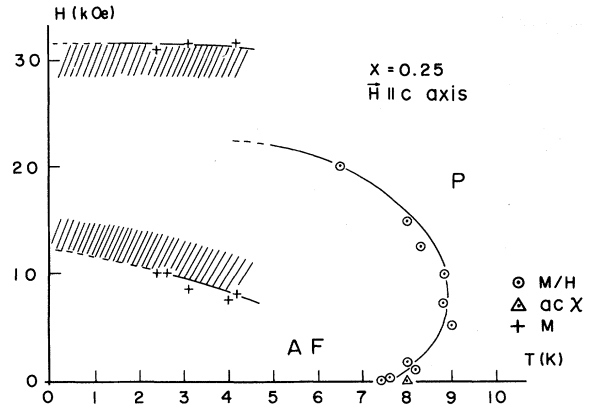

FIG. 11. Temperature—versus—external-magnetic-field phase diagram of the $x=0.25$ sample when the field is applied along the c axis. The transition region determined from the magnetization measurement is shown by the pluses. (P denotes paramagnetic and AF antiferromagnetic.)

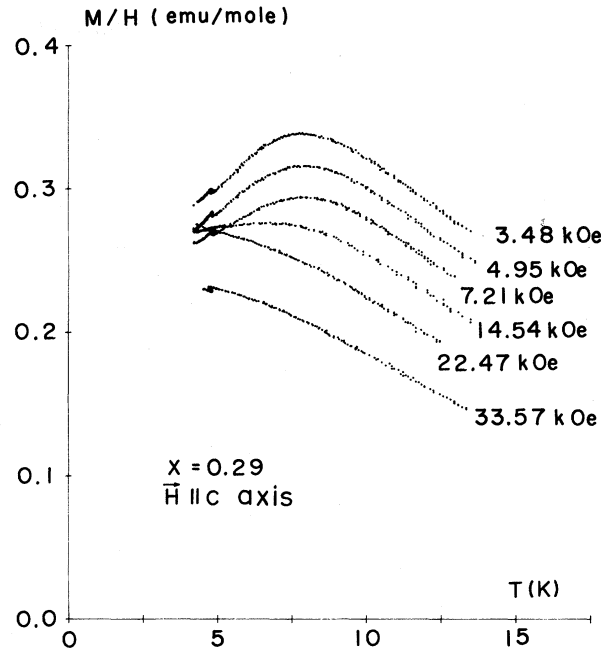

FIG. 12. Temperature dependence of the susceptibility along the c axis of the $x=0.29$ sample obtained under fixed external magnetic fields. The baseline of the susceptibility is downshifted by 0.02 emu/mol for each field. The baseline for the $H=3.48$ kOe is shown in the figure.

external field destroys the long-range order, and thus the system breaks into domains, the above argument is still applicable to the spin system inside the domains. The decrease of T_N above about 5 kOe is partly due to the random-field effect, but mainly results from the tricritical phase diagram similar to that observed in pure $FeBr_2$ (Refs. 25—27). The external-field—versus—temperature phase diagram of the $x=0.25$ sample obtained from the magnetization and susceptibility measurements is shown in Fig. 11. The Néel temperature increases with magnetic field up to about 5 kOe and then begins to decrease when the magnetic field is increased further. The transition region determined from the magnetization measurement is also shown in Fig. 11. The region is too wide to be explained by the sample demagnetizing field. This implies that the system is made up of different kinds of domains in the transition region.

Field dependence of the susceptibility-versus-temperature curve for the $x=0.29$ sample is shown in Fig. 12 for the magnetic field applied along the c axis. In this case, since the susceptibility curve is already rounded at zero field [Fig. 3(a)], the effect of external field is not so appreciable. The susceptibility decreases monotonically with increasing temperature for external magnetic fields above about 22 kOe. Thus the temperature—versus—magnetic-field phase diagram for the low-temperature phase transition in the $x=0.29$ sample seems to be still tricritical, as in the $x=0.25$ crystal (Fig. 11).

VII. DISCUSSION

We first discuss the absence of the phase boundary at L_3 and the dulling of the L_4 line described in Sec. IV. Matsubara and Inawashiro[4] have analyzed, in the molecular-field approximation, the magnetic properties of the random mixture with competing anisotropies, $Co_xNi_{1-x}Cl_2\cdot 6H_2O$, in which no low-temperature phase boundary has been observed.[35] The spin easy axes of $CoCl_2\cdot 6H_2O$ and $NiCl_2\cdot 6H_2O$ are not orthogonal (the angle between the axes is 115°). This configuration of the easy axes inevitably produces a nondiagonal coupling between the spin components of the form $-DS^zS^x\sin\gamma\cos\gamma$, where D is the single-ion anisotropy parameter and γ is the angle between the easy axes. The theoretical concentration—versus—transition-temperature phase diagram is such that there is only one phase boundary between the paramagnetic and antiferromagnetic phase. The spin direction in the antiferromagnetic phase changes with concentration continuously from that of $NiCl_2\cdot 6H_2O$ to that of $CoCl_2\cdot 6H_2O$. Because the easy axis of $FeBr_2$ is perpendicular to that of $CoBr_2$, the Matsubara-Inawashiro mechanism is not operative in our alloy. In the case when a nondiagonal exchange coupling between the spin components exists, the two low-temperature phase boundaries are expected to disappear in the molecular-field approximation even if the easy axes are orthogonal. As discussed by Wong *et al.*,[18] Fe^{2+} spins in $FeCl_2$ have a nondiagonal exchange interaction between them due to the degenerate orbital states. The same is true for Co^{2+} spins in $CoCl_2$. In the pure materials, the nondiagonal exchange interactions vanish by symmetry. In the mixed system $Fe_{1-x}Co_xCl_2$, on the other hand, the symmetry is locally broken and, as a result, a nondiagonal exchange interaction which is site random is produced. Since the crystal structures of the chlorides and bromides are nearly the same, we expect that the random nondiagonal exchange interactions are also present in $Fe_{1-x}Co_xBr_2$. As there is no theoretical study available, except that based on the random-field model, which takes into account the difference between Ising and XY characters, we discuss the absence of the line L_3 and the dulling of the line L_4 within the framework of the random-field

model. The line L_3 corresponds to the ordering of the XY component of the spins. The random field of the form $\tilde{J}\langle S^{\parallel}\rangle/\mu_B$ will destroy the ordering of the $S^{\perp}$ component since the mixed crystal $Fe_{1-x}Co_xBr_2$ is a three-dimensional magnet. The line L_4 represents the ordering of the Ising component. Because the strength of the random field does not differ much with concentration near x_M, the dulling of the transition at L_4 means that the lower critical dimension d_c of the Ising system is, at least, less than four ($d_c<4$). If $d_c=2$, then we should observe a sharp transition at L_4 in our mixed crystal. From the present results, therefore, the d_c value for the Ising system seems to be three.

We have observed that the external magnetic field applied along the c axis of $Fe_{1-x}Co_xBr_2$ in the Fe-rich concentration region causes the transition at L_1 to be less sharp [Fig. 10(a)]. Since the transition at L_1 under external field is modeled by an Ising transition under a random field, the above observation suggests again that the d_c value for the Ising system is three. In the case of diluted antiferromagnets, many experimental observations[19] seem also to show that the d_c value for the Ising model is three.

One question arises, then, why the line L_3 in Fig. 6 is absent in $Fe_{1-x}Co_xBr_2$ and is observed in $Fe_{1-x}Co_xCl_2$. One possible explanation for this within the random-field model would be that the size of the domains in which the XY spin components are correlated is larger in $Fe_{1-x}Co_xCl_2$ than in $Fe_{1-x}Co_xBr_2$. However, Oku and Igarashi[36] recently proposed an alternative explanation for this. They claimed that the random off-diagonal anisotropy,[37] rather than the random field, is an important factor in the transition at the low-temperature phase boundaries. They showed that the phase diagram given in Fig. 6 is possible when the random anisotropy is large. In order to clarify this situation, a microscopic calculation of the nondiagonal exchange interactions and the nondiagonal anisotropies is necessary. It is also important to perform a mean-field-type calculation of the phase diagram which is able to take into account the Ising and XY characters explicitly (e.g., Bethe approximation).

ACKNOWLEDGMENTS

We would like to express our sincere thanks to Professor R. J. Birgeneau, Professor T. Oguchi, Professor A. Ito, Dr. F. Matsubara, and Dr. M. Oku for their many helpful discussions and comments, and to the Toray Research Center for the chemical analysis. The work performed in Japan was partially supported by a Grant-in-Aid for Scientific Research from the Ministry of Education, Science and Culture and by the Yamada Science Foundation. The Laboratoire des Propriétés Mécaniques Thermodynamiques des Matériaux is associated with the Centre National de la Recherche Scientifique.

*Present address: Laboratoire de Dispositifs Infra-rouge, Tour 12, Université Pierre et Marie Curie, 4 Place Jussieu, 75230 Paris Cedex 05, France.

[1]For details, see A. Aharony, J. Magn. Magn. Mater. **31-34**, 1432 (1983), and references cited therein.

[2]For details, see K. Katsumata, J. Magn. Magn. Mater. **31-34**, 1435 (1983), and references cited therein.

[3]P. A. Lindgård, Phys. Rev. B **14**, 4074 (1976); **16**, 2168 (1977).

[4]F. Matsubara and S. Inawashiro, J. Phys. Soc. Jpn. **42**, 1529 (1977); **46**, 1740 (1979); **47**, 1102 (1979).

[5]T. Oguchi and T. Ishikawa, J. Phys. Soc. Jpn. **45**, 1213 (1978).

[6]Y. Someya, J. Phys. Soc. Jpn. **50**, 3897 (1981).

[7]A. Aharony and S. Fishman, Phys. Rev. Lett. **37**, 1587 (1976).

[8]S. Fishman and A. Aharony, Phys. Rev. B **18**, 3507 (1978).

[9]K. Katsumata, M. Kobayashi, T. Satō, and Y. Miyako, Phys. Rev. B **19**, 2700 (1979).

[10]M. Kobayashi, K. Katsumata, T. Satō, and Y. Miyako, J. Phys. Soc. Jpn. **46**, 1467 (1979).

[11]K. Katsumata, M. Kobayashi, and H. Yoshizawa, Phys. Rev. Lett. **43**, 960 (1979).

[12]K. Katsumata, H. Yoshizawa, G. Shirane, and R. J. Birgeneau (unpublished).

[13]T. Tawaraya and K. Katsumata, Solid State Commun. **32**, 337 (1979).

[14]T. Tawaraya, K. Katsumata, and H. Yoshizawa, J. Phys. Soc. Jpn. **49**, 1299 (1980).

[15]Po-zen Wong, P. M. Horn, R. J. Birgeneau, C. R. Safinya, and G. Shirane, Phys. Rev. Lett. **45**, 1974 (1980).

[16]A. Ito, S. Morimoto, Y. Someya, H. Ikeda, Y. Syono, and H. Takei, Solid State Commun. **41**, 507 (1982).

[17]A. Ito, S. Morimoto, Y. Someya, Y. Syono, and H. Takei, J. Phys. Soc. Jpn. **51**, 3173 (1982).

[18]P. Wong, P. M. Horn, R. J. Birgeneau, and G. Shirane, Phys. Rev. B **27**, 428 (1983).

[19]For details, see R. J. Birgeneau, R. A. Cowley, G. Shirane, and H. Yoshizawa, J. Stat. Phys. (to be published), and references cited therein.

[20]K. Katsumata, J. Tuchendler, and S. Legrand, Solid State Commun. **49**, 83 (1984).

[21]M. K. Wilkinson, J. W. Cable, E. O. Wollan, and W. C. Koehler, Phys. Rev. **113**, 497 (1959).

[22]M. C. Lanusse, P. Carrara, A. R. Fert, G. Mischler, and J. P. Redoulès, J. Phys. (Paris) **33**, 429 (1972).

[23]W. B. Yelon and C. Vettier, J. Phys. C **8**, 2760 (1975).

[24]H. Yoshizawa, K. Ubukoshi, and K. Hirakawa, J. Phys. Soc. Jpn. **48**, 42 (1980).

[25]I. S. Jacobs and P. E. Lawrence, J. Appl. Phys. **35**, 996 (1964).

[26]A. R. Fert, P. Carrara, M. C. Lanusse, G. Mischler, and J. P. Redoulès, J. Phys. Chem. Solids **34**, 223 (1973).

[27]T. E. Wood, A. Muirhead, and P. Day, J. Phys. C **11**, 1619 (1978).

[28]J. Magariño, J. Tuchendler, A. R. Fert, and J. Gelard, Solid State Commun. **23**, 175 (1977).

[29]K. Katsumata and M. Kobayashi, Kotai Butsuri **13**, 41 (1978).

[30]M. E. Fisher, Philos. Mag. **7**, 1731 (1962).

[31]L. Bevaart, E. Frikkee, J. V. Lebesque, and L. J. de Jongh, Solid State Commun. **25**, 539 (1978); Phys. Rev. B **18**, 3376 (1978).

[32]L. Bevaart, E. Frikkee, and L. J. de Jongh, Solid State Commun. **25**, 1031 (1978); Phys. Rev. B **19**, 4741 (1979).

[33]I. Yamamoto, J. Phys. Soc. Jpn. **49**, 74 (1980).

[34]S. Fishman and A. Aharony, J. Phys. C **12**, L729 (1979).

[35]K. Takeda, M. Matsuura, and T. Haseda, J. Phys. Soc. Jpn. **29**, 885 (1970).

[36]M. Oku and H. Igarashi, Prog. Theor. Phys. **70**, 1493 (1983).

[37]D. Mukamel and G. Grinstein, Phys. Rev. B **25**, 381 (1982).